Int. J. Radiation Oncology Biol. Phys., Vol. 71, No. 2, pp. 484–490, 2008

0360-3016/08/$–see front matter

doi:10.1016/j.ijrobp.2007.11.046

**CLINICAL INVESTIGATION** **Brain**

# HIGH-DOSE, SINGLE-FRACTION IMAGE-GUIDED INTENSITY-MODULATED RADIOTHERAPY FOR METASTATIC SPINAL LESIONS

Yoshiya Yamada, M.D., F.R.C.P.C.,* Mark H. Bilsky, M.D.,† D. Michael Lovelock, Ph.D.,‡ Ennapadam S. Venkatraman, Ph.D.,§ Sean Toner, M.S.,‡ Jared Johnson, B.S.,* Joan Zatcky, N.P.,* Michael J. Zelefsky, M.D.,* and Zvi Fuks, M.D.*

Departments of *Radiation Oncology, †Neurosurgery, ‡Medical Physics, and §Biostatistics, Memorial Sloan-Kettering Cancer Center, New York, NY

**Purpose:** To report tumor control and toxicity for patients treated with image-guided intensity-modulated radiotherapy (RT) for spinal metastases with high-dose single-fraction RT.

**Methods and Materials:** A total of 103 consecutive spinal metastases in 93 patients without high-grade epidural spinal cord compression were treated with image-guided intensity-modulated RT to doses of 18–24 Gy (median, 24 Gy) in a single fraction between 2003 and 2006. The spinal cord dose was limited to a 14-Gy maximal dose. The patients were prospectively examined every 3–4 months with clinical assessment and cross-sectional imaging.

**Results:** The overall actuarial local control rate was 90% (local failure developed in 7 patients) at a median follow-up of 15 months (range, 2–45 months). The median time to local failure was 9 months (range, 2–15 months) from the time of treatment. Of the 93 patients, 37 died. The median overall survival was 15 months. In all cases, death was from progression of systemic disease and not local failure. The histologic type was not a statistically significant predictor of survival or local control. The radiation dose was a significant predictor of local control ($p = 0.03$). All patients without local failure also reported durable symptom palliation. Acute toxicity was mild (Grade 1-2). No case of radiculopathy or myelopathy has developed.

**Conclusion:** High-dose, single-fraction image-guided intensity-modulated RT is a noninvasive intervention that appears to be safe and very effective palliation for patients with spinal metastases, with minimal negative effects on quality of life and a high probability of tumor control. 

**Image-guided radiotherapy, Single fraction, Spinal metastases, Intensity-modulated radiotherapy.**

## INTRODUCTION

Radiotherapy (RT) is generally delivered by fractionated, rather than single-dose, schemes. Fractionated RT was developed early in the 20th century, when it was realized that treatment uncertainties required inclusion of large safety margins of normal tissue (~2 cm around the tumor), frequently resulting in unacceptable treatment toxicities at the single dose levels required for tumor response (1, 2). Fractionated RT differentially protects normal tissue stem cells because of the more proficient DNA damage repair during interfraction intervals (3), thus enabling, in many patients, the assembly of cumulative target doses sufficient for local tumor cure, while conferring just-acceptable normal tissue morbidity (4).

The introduction of computed tomography (CT)-based treatment planning and portal imaging of treatment fields has decreased the magnitude of the treatment uncertainties, permitting a reduction of the normal tissue margins. When combined with high-precision tumor targeting using stereotactic technology, it has enabled the safe delivery of single-dose RT to intracranial lesions (generically termed stereotactic radiosurgery [SRS]), using minimal safety margins of ≤2 mm that do not result in clinically relevant damage in the surrounding brain tissue (5, 6). Early studies of single-dose SRS for oligometastatic brain tumors demonstrated dose-dependent local tumor control, with a freedom from local relapse rate at 1–2 years after 15–18 Gy of approximately 50% and ≥80% after 22–24 Gy, regardless of the histologic tumor phenotype (7–9). However, the long-term local outcome of treated lesions remains unknown, because most patients succumb to progressive extracranial disease, frequently in the presence of apparent locally controlled intracranial lesions.

The first-generation SRS techniques have been mostly appropriate for treatment of small spherical tumors ≤3 cm in diameter (10). Treatment has involved multiple circular

Reprint requests to: Yoshiya Yamada, M.D., F.R.C.P.C., Department of Radiation Oncology, Memorial Sloan-Kettering Cancer Center, 1275 York Ave., New York, NY 10021. Tel: (212) 639-2950; Fax: (212) 639-2417; E-mail: yamadaj@mskcc.org

Conflict of interest: Y. Yamada participated in the Speaker's Bureau of Varian Medical Systems in 2007. None of the other authors have any conflicts of interest to disclose.

Received Aug 27, 2007, and in revised form Nov 27, 2007. Accepted for publication Nov 30, 2007.

overlapping fields or arrays of arcing coplanar or noncoplanar beams to construct a sphere of high radiation dose completely covering the planning treatment volume (PTV) with the prescribed dose. However, in larger or irregular tumor volumes, these techniques produce tumor dose inhomogeneities and loss of normal tissue sparing because of gradual falloff of the prescribed dose at the target edge and the peritumoral normal tissues (8, 11, 12). Accordingly, it has been reported that high-dose SRS (>15 Gy) of large (>3 cm in diameter) metastatic brain tumors resulted in substantial volumes of normal brain tissue exposed to potentially toxic radiation doses, requiring tumor dose reduction to avoid unacceptable complication risks (10, 12).

To overcome these deficiencies, the current SRS techniques use image-guided robotic technology to alter the position and trajectory of the beam delivery system (13) or micro-multileaf collimated beams designed by inverse planning to generate intensity-modulated RT (IMRT) (8, 11, 14). The treatment plans tightly conform the prescribed dose to the tumor, while featuring steep dose gradients at the PTV edge and the immediate surrounding normal tissues. The new systems have enabled the application of stereotactic body RT to extracranial oligometastatic tumors with hypofractionated or single high-dose exposures (15). Single-dose stereotactic body RT for oligometastatic tumors to the liver (16, 17) and lung (18–20) have confirmed the advantage of high, single-dose therapy (20–30 Gy) over lower dose levels in effecting long-term local control, regardless of the tumor histologic phenotype. Although the survival of patients frequently enables long-term outcome evaluations, concerns still exist regarding the quality of treatment delivery to liver and lung tumors, and hence of the actual dose used, because of the treatment uncertainties associated with respiratory motion of the target. Evaluations of the dose–response patterns would likely be more dependable in static organs, such as the head and neck, limbs, bone, and retroperitoneum.

We recently reported on the feasibility and safety of a stereotactic intensity-modulated beam technique to treat spinal metastatic tumors using on-line treatment field imaging to ensure the precision of tumor targeting (image-guided IMRT) (21, 22). The treatment of these tumors presents a particular challenge because of the close proximity to the spinal cord and residing frequently within a concave-shaped target volume. IMRT is particularly suited for the treatment of such complex anatomic features, but it requires a high degree of precision in tumor targeting, which can be provided by on-line image guidance. Our data showed this approach enabled curative homogeneous fractionated dose distributions in large PTVs (44–316 $cm^3$, equivalent to spherical diameters of 4–9 cm), with dose sparing of nearby critical structures, such that the spinal cord did not exhibit radiation toxicity (22). We now report the results of using high-dose (18–24 Gy), single-fraction image-guided IMRT in 93 consecutive patients with metastatic tumors to the spine of different histologic types. The data indicated a 90% rate of local control, regardless of the histologic phenotype, without transgressing spinal cord tolerance dose levels and without evidence of significant acute toxicity or long-term morbidity. The results of this study have indicated that coupling IMRT and image-guided RT (IGRT) provides a powerful clinical approach to curative treatment of irregularly shaped large-volume tumors within close proximity to the spinal cord and other dose-sensitive normal structures with single-dose RT.

## METHODS AND MATERIALS

All patients had a histologically confirmed diagnosis of solid tumor malignancy, with radiologic evidence of metastasis to the spine. The patients were reviewed in a multidisciplinary fashion by the institutional spinal tumor board, consisting of neurosurgeons, orthopedic surgeons, neuroradiologists, and physiatrists. No patient had undergone surgical resection of the lesion of interest. Patients were excluded from this study if they had high-grade epidural cord compression, mechanical instability, or a history of RT to the region of interest. All patients were immobilized in a noninvasive customized cradle developed at our institution for image-guided IMRT (21). Four spherical infrared reflectors were placed on the patient below and above the region of interest at treatment. These reflectors were tracked with infrared stereoscopic cameras to monitor intrafraction patient movement. If motion >2 mm was noted, the treatment was stopped, and the positioning was verified again with both two-dimensional and three-dimensional imaging. Patient motion that exceeded the 2-mm threshold was observed on two occasions, and these patients were successfully repositioned.

The techniques used for treatment planning and delivery of image-guided IMRT at our institution have been previously described (21, 22). Patients underwent treatment simulation in the cradle using CT images with a 2-mm slice thickness. The spinal cord was outlined using either myelograms the day of simulation or magnetic resonance imaging fusion, with the patients immobilized in the cradle for image acquisition.

Treatment planning was done on in-house software with inverse treatment algorithms for all patients in the same manner. The prescribed doses ranged from 18 to 24 Gy to the PTV (23). The PTV was created by expanding the clinical tumor volume $\geq$2 mm. In the case of vertebral body involvement, the clinical tumor volume included the entire vertebral body. The PTV was never allowed to violate the spinal cord contour in cases in which epidural disease extension was present. Dose constraints of 12–14 Gy were set as the maximal allowable dose to the spinal cord contour. Typically, seven to nine coplanar fields were set to a single isocenter using dynamic multileaf collimation. The doses in all cases were prescribed to the 100% isodose line. This was determined using a standardized best fit inverse optimization process, taking into account normal tissue constraints and gross tumor volume, clinical tumor volume, and PTV coverage. In each case, the plan was normalized to the 100% isodose line to maximize the percentage of the PTV that received 100% of the prescribed dose without exceeding the maximal allowable spinal cord or cauda equina dose limits. Treatment was delivered with 6-MV and/or 15-MV photons. Higher energy photons were typically chosen for deeper lesions, such as those in the lumber spine. Mixed energies were used for some patients.

Digitally reconstructed radiographs from the simulation studies were created for each field's beam's eye view, which were used as the reference images for targeting the tumor with on-line imaging during treatment. Digital megavoltage portal imaging or kilovoltage imaging was obtained after the patient was positioned in the cradle on the treatment couch. These images were digitally overlayed with the reference digitally reconstructed radiographs to calculate the

isocenter corrections. The calculated corrections were then verified for each field by on-line portal images before actual treatment.

Linear accelerator gantry-mounted cone-beam CT (CBCT) was incorporated into the verification process in 2004. No differences in accuracy between CBCT and megavoltage imaging used before 2004 were noted (within 2 mm). A pretreatment CBCT scan was obtained immediately before treatment. Any differences in the target position relative to the treatment planning CT scan was corrected and verified with another CBCT scan and two-dimensional kilovoltage imaging before initiating treatment. A CBCT scan was also obtained to verify positioning after treatment was completed.

Patients were pretreated with dexamethasone to prevent acute treatment-related edema and pain. All patients were examined 8 weeks after treatment with repeat magnetic resonance imaging and every 3–4 months thereafter. Treatment failure was defined as disease progression confirmed on magnetic resonance imaging.

Estimates of overall survival were calculated using the Kaplan-Meier method (24). The cumulative incidence curves for the time to local failure were obtained using the competing risks method (25) because a significant number of patients (n = 37, 39%) had died, and 36 patients had died of systemic disease progression without apparent local failure. The histologic type was not a statistically significant factor in the probability of local failure.

## RESULTS

A total of 93 consecutive patients with 103 lesions underwent high-dose, single-fraction image-guided IMRT between July 2003 and December 2006. The median follow-up was 15 months (range, 2–45). Three patients were lost to follow-up at 8, 10, and 18 months after treatment, without evidence of local failure at their last follow-up visit. The clinical characteristics are summarized in Table 1.

The most frequent lesions treated were metastatic tumors of gastrointestinal origin (n = 22) or from the kidney (n = 21), followed by 13 prostate cancer and 13 sarcoma lesions. Of the 93 patients, 16% had not undergone previous systemic therapy before treatment, and 13% had not undergone any systemic therapy at last follow-up. The use of systemic therapy did not affect either local control or survival.

Table 1. Patient characteristics

| Characteristic | Value |
|---|---|
| Age (y) | |
| Range | 38–91 |
| Median | 62 |
| Follow-up (mo) | |
| Range | 6–36 |
| Median | 15.7 |
| Histologic type | |
| Breast | 6 |
| Cholangiocarcinoma | 6 |
| Colon cancer | 11 |
| Hemangiopericytoma | 2 |
| Hepatocellular cancer | 4 |
| Sarcoma | 10 |
| Melanoma | 15 |
| Non–small-cell lung cancer | 5 |
| Paraganglionoma | 1 |
| Prostate cancer | 13 |
| Renal cell cancer | 21 |
| Salivary gland cancer | 2 |
| Thyroid cancer | 5 |
| Squamous cell cancer (tonsil) | 1 |
| Bladder | 1 |

### *Local control*

The actuarial local control rate using the Kaplan-Meier method was 90% (Fig. 1). Seven patients developed local failure, two with prostate tumors, two with renal cell carcinoma, and one each with adenoid cystic carcinoma, colorectal carcinoma, and melanoma. None of the patients with breast, lung, or sarcoma developed a local failure. The estimated cumulative incidence of local failure, taking death into account, using death as a competing risk factor to local control, was 7.5% at 24 months (Fig. 2). The median follow-up for patients with treatment failure after single-fraction RT was 22 months (range, 10–45). Three patients with local recurrence died. In these 3 patients, the local recurrence was initially successfully salvaged surgically, and 2 of the 3 patients died 5–8 months after surgery of progressive systemic disease without local failure. The third patient died 12 months after treatment with active disease recurrence at the treatment site. One patient with metastatic prostate cancer underwent salvage surgery that failed and then underwent repeat image-guided IMRT (IGRT, 3,000 cGy in five fractions) and was without evidence of recurrence 6 months after RT. Salvage surgery and salvage IGRT failed in an additional patient with adenoid cystic carcinoma of the parotid gland.

The 45-month actuarial survival rate of this group was 36%. Of the 93 patients, 37 have died, and the median time to death from the time of treatment was 10 months (range, 1–39). All deaths were attributed to progression of systemic disease, and all but 1 of these patients had no evidence of local failure at death.

### *Effect of dose*

A prescribed dose of <2,300–2,400 cGy (2,400 cGy vs. <2,400 cGy, $p = 0.03$; >2,300 cGy vs. <2,300 cGy, $p = 0.04$) was significantly associated statistically with local failure (Fig. 3). Two patients who were treated to a dose of 2,400

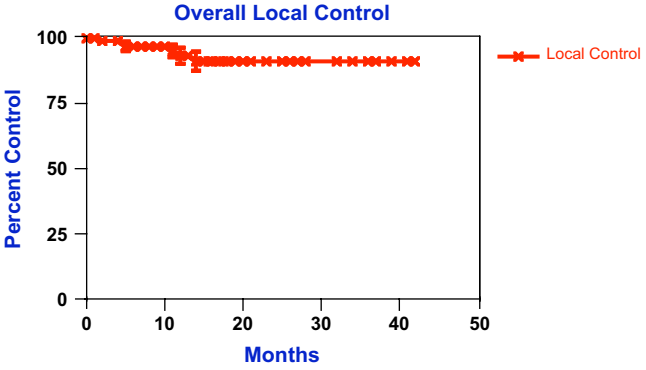


Fig. 1. Actuarial local control (Kaplan-Meier method). Y axis represents probability of local control.

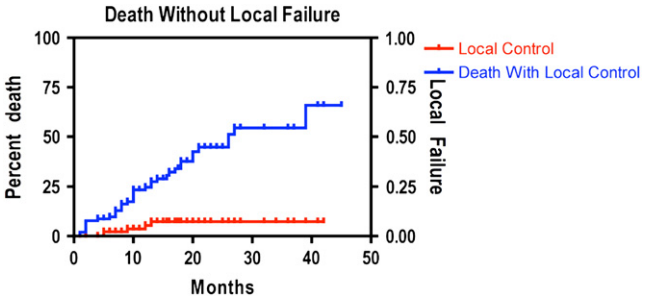


Fig. 2. Cumulative probability of local failure and death without local failure, taking into account death as competing risk to local failure.

cGy had treatment failure 2 and 12 months after treatment. The mean dose of the patients with failure after lower dose treatment was 2,080 cGy. The mean time to failure in the low-dose cohort was 8.2 months (range, 5–13). Patients with no evidence of disease progression did not exhibit relapse of the original presenting symptoms.

Figure 4 represents a typical response to treatment. The patient had an epidural colorectal metastasis at T8 and pain not well managed with medical therapy. The pain had completely resolved within 10 days of delivery of a single treatment of 21 Gy, when the patient discontinued all pain medications. This patient had no evidence of recurrence in the treated field.

*Oligometastatic status*

The specific global metastatic status was available in detail for 70 patients, and all patients had had a systemic disease assessment within 2 months before RT (minimum of a bone scan and CT of the chest abdomen pelvis, or positron emission tomography scan). Most patients ($n = 67$; 96%) had oligometastatic disease (three or fewer synchronous metastases) at treatment. At the last follow-up visit, 28 patients (42%) had evidence of more than three metastases (progressive systemic

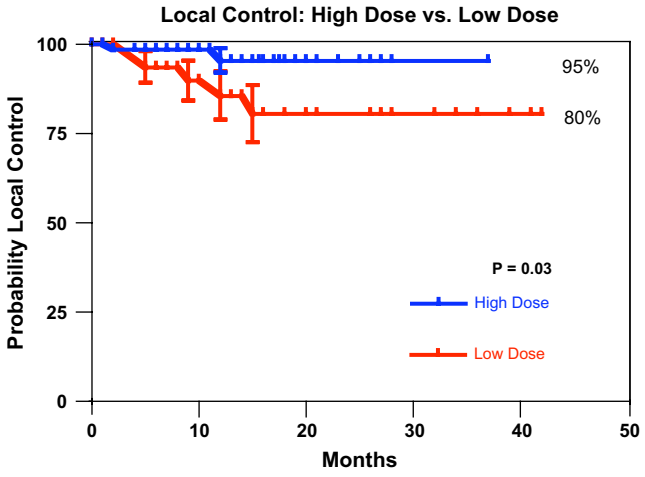


Fig. 3. Local control probability by dose. Statistically significant difference noted for patients treated to 2,400 cGy vs. 1,800–2,300 cGy.

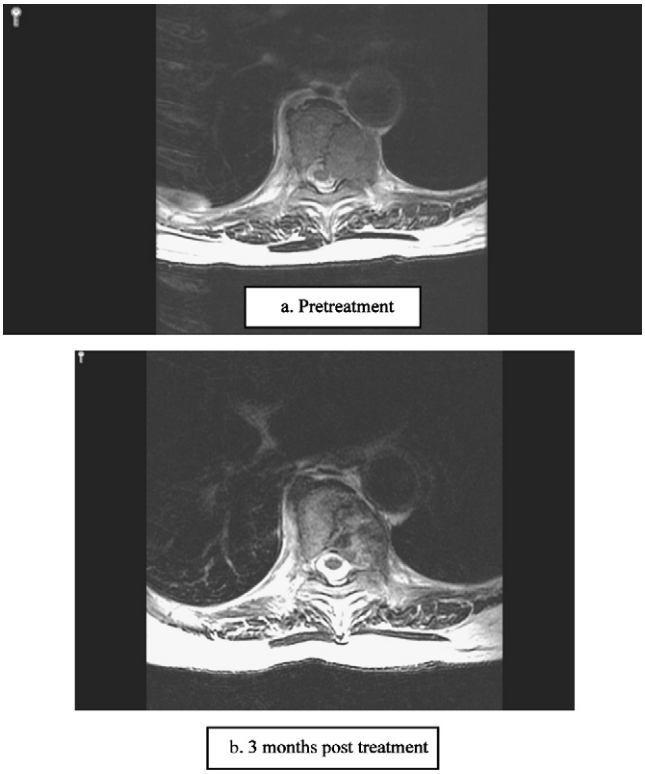


Fig. 4. (a) Before and (b) after treatment images 8 weeks after treatment. Patient had received 2,100 cGy in single fraction. Soft-tissue component of tumor, both paraspinal and epidural, had decreased in size.

disease). Overall, the actuarial probability of remaining oligometastatic was 33%. When analyzed by histologic type, breast cancer and head-and-neck cancer patients had the greatest actuarial rates of remaining oligometastatic (67% and 80%, respectively) and the greatest rates of survival (100%). An intermediate group consisting of prostate cancer, sarcoma, and melanoma patients remained oligometastatic (range, 59–65%), with similar survival rates. Renal, gastrointestinal, and lung cancer patients faired the worst. In this group, <35% remained oligometastatic. For the renal and gastrointestinal cancer patients, the actuarial survival rate was 36% and 16%, respectively. Oligometastatic status and survival by histologic type are summarized in Table 2.

In 4 patients, the site of treated disease was the only site of demonstrated metastasis (renal, colorectal, prostate, and head-and-neck primary tumor). One patient with prostate cancer had no evidence of another metastasis 10.7 months after treatment. The remainder of the patients developed additional metastases but remained oligometastatic at a median follow-up of 18.7 months (range, 10–29). All patients in this group were alive at the last follow-up, and no patient developed recurrence at the site of single-fraction image-guided IMRT. The median time to development of additional metastases was 10.6 months (range, 3.8–18.5) In patients who had two to three metastases at treatment, the median time to progression beyond oligometastases was 8.5 months (range, 1–25.6).

Table 2. Oliogometastatic progression

| Histologic type | Patients with >3 metastases | Median time to progression (mo) | Probability of progression (%) | Median follow-up (mo) | Survival (%) |
|---|---|---|---|---|---|
| Head and neck | 1/8 | 11.5 | 20 | 20.7 | 100 |
| Breast | 1/3 | 12 | 33 | 12 | 100 |
| Prostate | 4/11 | 11.2 | 41 | 18.3 | 92 |
| Sarcoma | 2/8 | 9.3 | 35 | 12 | 66 |
| Melanoma | 3/8 | 6.6 | 37 | 15.2 | 60 |
| Lung | 5/7 | 8.8 | 79 | 15 | 100 |
| Renal | 5/10 | 7.7 | 76 | 12 | 36 |
| Gastrointestinal | 4/10 | 11.6 | 65 | 16.4 | 16 |

*Dosimetry*

The dosimetric characteristics of this cohort are summarized in Table 3. The median prescribed dose to the PTV was 2,400 cGy (range, 1,800–2,400), with a maximal PTV dose of 2,604 cGy. Overall, near optimal coverage of the PTV was achieved, despite the close proximity of the spinal cord. The maximal dose to the spinal cord was constrained to <12–14 Gy as a maximal point dose to a single voxel of the spinal cord contour. This strict constraint resulted in lower doses to a small rim of epidural tissues to preserve the spinal cord limits. Nonetheless, the median percentage of the PTV that received ≥95% of the prescribed dose was 95% (range, 82–100%).

*Toxicity*

No patient experienced myelopathy or radiculopathy. No difference in any toxicity was noted whether the spinal cord was constrained to 12 or 14 Gy. One patient experienced severe pain 3 hours after RT that required hospitalization. Two patients had radiographic evidence of vertebral body fractures without evidence of tumor progression. Acute Grade 1-2 skin reactions were noted in 3 patients. Acute esophagitis requiring dietary modification (Grade 2) occurred in 2 patients. One patient developed tracheoesophageal fistula 9 months after RT in the approximate treatment region while receiving adriamycin-based chemotherapy that required surgical intervention. An adriamycin recall reaction might have contributed to the development of this complication. No apparent differences in esophageal dosimetry were noted. No other noteworthy toxicity has occurred.

Table 3. Dosimetric characteristics

| | |
|---|---|
| Prescribed dose *(n)* | |
| 1,800 cGy | 5 |
| 2,000 cGy | 2 |
| 2,100 cGy | 23 |
| 2,200 cGy | 5 |
| 2,300 cGy | 1 |
| 2,400 cGy | 67 |
| Median (cGy) | 2,400 |
| Mean (cGy) | 2,295 |
| Maximal spinal cord dose (cGy) | |
| Median | 1,167 |
| Range | 182–1,400 |
| Maximal cauda equina dose (cGy) | |
| Median | 987 |
| Range | 100–1,560 |
| PTV | |
| $D_{95}$ (%) | |
| Median | 100.1 |
| Range | 76.2–104.5 |
| $V_{95}$ (%) | |
| Median | 95.8 |
| Range | 81–100 |
| Volume ($cm^3$) | |
| Median | 65.8 |
| Range | 7.6–227 |

*Abbreviations:* PTV = planning target volume; $D_{95}$ = minimal dose received by 95% of target volume; $V_{95}$ = percentage of PTV that received 95% of prescribed dose.

## DISCUSSION

The results of the present study have confirmed single-dose RT as a powerful clinical approach for achieving long-term local control of human tumors. The relative benign patterns of metastatic progression and survival in our group of patients have enabled a valid evaluation of the local control conferred by RT for several metastatic tumor types. Previous studies of SRS for metastatic tumors to the brain, lung, and liver have indicated high local control rates in tumor lesions treated with doses >20 Gy (26–29). However, the overall short-term survival of patients in these series raised questions relative to the validity if these observations. Although most patients in the present study did develop further disease progression, even those who eventually died of their disease lived a median of 10 months after IGRT, most without local recurrence in the treated site. The median follow-up of the study cohort also exceeded the median time to failure. Thus, despite systemic disease progression, most patients appeared to have had sufficient survival to support the idea that high, single-dose RT (*i.e.,* 24 Gy) is potentially curative of local human tumors, regardless of the histologic tumor type.

The question of whether single-dose RT has curative potential for human tumors has been an issue of considerable controversy. The classic paradigms of radiobiology suggest that some fractionation might be required to account for tumor hypoxia, because fractionation affords the reoxygenation required to overcome hypoxia-mediated radioresistance (30). The fraction size can differ by the number of fractions, predicted by linear quadratic model calculations. However, although abundant animal and clinical data have confirmed that standard linear quadratic modeling performs well in

predicting the optimal fractionation parameters for treatments of ≥8 Gy/fraction, this model is inconsistent with the clinical outcomes noted for radiosurgery (31, 32).

Because the linear quadratic model assumes a specific radiation response mechanism, it could indicate that tissue stem cells exposed *in vivo* to fractions <8 Gy respond by a different mechanism than those exposed to >8–10 Gy. Recent work has challenged the prevailing hypothesis that tissue stem cell clonogens succumbing directly to reproductive cell death represent the only relevant targets in radiation-induced tissue damage (31). Using experimental mouse tumor models, these studies have provided evidence that the normal and tumor tissue stem cell response to high single-dose exposures (≥15 Gy) is conditionally linked to the induction of microvascular endothelial apoptosis in the targeted tissue, defining a two-target model. Genetic and pharmacologic manipulations that conferred the endothelium refractory to radiation-induced apoptosis converted the tissues completely resistant to lethal single-dose RT. Furthermore, both fractionated and single-dose RT appears capable of engaging a vascular component of the tumor response, albeit by different mechanisms that result in different outcomes. Hence, whether human tumors engage a vascular component in the tumor response to high single-dose RT, the present, and previously reported, observations that human tumors can be locally controlled with single doses of ~24 Gy, regardless of tumor type, are consistent with this hypothesis.

The natural history of bone metastasis is characterized by progressive destruction of bone by invading tumor and palliative treatment of bone metastases with RT has been widely studied. A meta-analysis of randomized trials, including 3,260 patients, that compared low-dose, single-fraction RT (median, 8 Gy) with fractionated schedules (median, 4 Gy × 5) for the treatment of bone metastases has been reported (32). In this analysis, although no significant difference was found between the use of low-dose, single-fraction RT and standard fractionation schedules in terms of clinical outcomes such as pain, a trend in favor of single-fraction RT (62% vs. 59%) was noted. Although single-fraction RT was used, the relatively low doses reported (compared with the doses given in the present report) might have accounted for the lack of a significant difference in pain improvement.

Also, limited published data are available on the outcome of fractionated RT for the management of spinal metastases. Investigators from Nagoya University published a retrospective analysis of 101 patients with spinal metastases; 95% of the patients were treated with 40 Gy in 20 fractions (33). With a cumulative survival rate of 45% at 1 year, only 20% had experienced durable pain relief. Maranzano *et al.* (34) reported on a trial of patients with metastatic cord compression, randomizing 8 Gy × 2 within 1 week vs. a split course of 5 Gy × 3 plus 3 Gy × 5. With a median follow-up of 33 months, 56% of the short-course and 59% of the split-course patients experienced pain relief. No survival differences were observed. Patchell *et al.* (35) reported a Phase III trial comparing surgical resection and RT (3 Gy × 10) vs. RT alone (3 Gy × 10) in patients with high-grade spinal cord compression (35). The patients who received fractionated RT alone did significantly worse in all functional categories, underscoring the limited utility of fractionated RT alone in the management of locally aggressive spinal metastases.

In contrast to the relatively disappointing outcomes reported with conventional fractionation or low-dose single-fraction RT, high-dose, single-fraction RT was shown to be highly effective in the palliation of metastatic spinal cord tumors. Gerszten and Welch (36) reported on 500 patients with paraspinal lesions treated with 12–25 Gy (maximal intratumoral dose) single-fraction RT. SRS was the primary treatment modality for the spinal lesion in 65 patients. The control of symptoms was excellent; 86% reported improvement in pain, and 90% were reported to have local control. Toxicity was minimal, including no treatment-related myelopathy (36). Gerszten *et al.* (37) also recently reported the results of 60 patients with renal cell cancer histologic features. With a median follow-up of 37 months, 90% of the patients reported long-term palliation, and no myelopathy was noted (37). Similar favorable results have also been reported by the Stanford University group (38) and are consistent with our results in the present report.

There are many important corollaries to our approach to treat paraspinal tumors with high-dose, single-fraction, image-guided IMRT. Because the spine is quite stable, it can be reliably immobilized to the similar tolerances expected with intracranial radiosurgery (21). The histologic types considered relatively radioresistant to fractionated RT such as melanoma and renal cell carcinoma have responded very favorably to single-fraction cranial radiosurgery (39, 40). Our experience with high-dose, single-fraction spinal image-guided IMRT has mirrored the experience of intracranial radiosurgery, suggesting that high-dose, single-fraction RT is efficacious both intra- and extracranially. Single-fraction, paraspinal image-guided IMRT has been well tolerated. In particular, neural tissues, including spinal nerve roots, which often received the prescription dose, seemed to tolerate high-dose RT without sequelae.

## CONCLUSION

The delivered radiation dose does appear to make a difference. With image-guided treatment verification, errors can be minimized to within 2 mm (21). This level of accuracy has enabled the delivery of high-dose, single-fraction RT within close proximity to the spinal cord without toxicity. IMRT is ideally suited to creation of the concave dose distributions necessary for cord-sparing treatment plans. Image-guided verification provides a mechanism to minimize the uncertainties associated with traditional RT. The coupling of IMRT and image-guided techniques takes full advantage of the extremely conformal potential of IMRT to provide high-dose RT with low normal tissue exposure and a high degree of confidence. The experience reported for high-dose, single-fraction image-guided RT is proof of principle that improved treatment accuracy has resulted in improved outcomes, with minimal serious morbidity.

## REFERENCES


1. Coutard H. Principles of X-ray therapy of malignant disease. *Lancet* 1934;2:1–12.
2. Bernier J, Hall EJ, Giaccia A. Radiation oncology: A century of achievements. *Nat Rev Cancer* 2004;4:737–747.
3. Lett J, Adler H, editors. Advances in radiation biology. Vol 5. New York: Academic Press; 1975. p. 241–271.
4. Okunieff P, Morgan D, Niemierko A, *et al*. Radiation dose-response of human tumors. *Int J Radiat Oncol Biol Phys* 1995; 32:1227–1237.
5. Corn BW, Curran WJ Jr., Shrieve DC, *et al*. Stereotactic radiosurgery and radiotherapy: New developments and new directions. *Semin Oncol* 1997;24:707–714.
6. Leksell L. The stereotaxic method and radiosurgery of the brain. *Acta Chir Scand* 1951;102:316–319.
7. Shiau CY, Sneed PK, Shu HK, *et al*. Radiosurgery for brain metastases: relationship of dose and pattern of enhancement to local control. *Int J Radiat Oncol Biol Phys* 1997;37:375–383.
8. Shiu AS, Kooy HM, Ewton JR, *et al*. Comparison of miniature multileaf collimation (MMLC) with circular collimation for stereotactic treatment. *Int J Radiat Oncol Biol Phys* 1997;37: 679–688.
9. Vogelbaum MA, Angelov L, Lee SY, *et al*. Local control of brain metastases by stereotactic radiosurgery in relation to dose to the tumor margin. *J Neurosurg* 2006;104:907–912.
10. Shaw E, Scott C, Souhami L, *et al*. Single dose radiosurgical treatment of recurrent previously irradiated primary brain tumors and brain metastases: Final report of RTOG protocol 90-05. *Int J Radiat Oncol Biol Phys* 2000;47:291–298.
11. Marks LB, Sherouse GW, Das S, *et al*. Conformal radiation therapy with fixed shaped coplanar or noncoplanar radiation beam bouquets: A possible alternative to radiosurgery. *Int J Radiat Oncol Biol Phys* 1995;33:1209–1219.
12. Nedzi LA, Kooy H, Alexander E III, *et al*. Variables associated with the development of complications from radiosurgery of intracranial tumors. *Int J Radiat Oncol Biol Phys* 1991;21: 591–599.
13. Adler JR Jr., Chang SD, Murphy MJ, *et al*. The Cyberknife: A frameless robotic system for radiosurgery. *Stereotact Funct Neurosurg* 1997;69:124–128.
14. Cosgrove VP, Jahn U, Pfaender M, *et al*. Commissioning of a micro multi-leaf collimator and planning system for stereotactic radiosurgery. *Radiother Oncol* 1999;50:325–336.
15. Song DY, Kavanagh BD, Benedict SH, *et al*. Stereotactic body radiation therapy: Rationale, techniques, applications, and optimization. *Oncology (Williston Park)* 2004;18:1419–1430; discussion 1430, 1432, 1435, 1416.
16. Herfarth KK, Debus J, Lohr F, *et al*. Stereotactic single-dose radiation therapy of liver tumors: Results of a phase I/II trial. *J Clin Oncol* 2001;19:164–170.
17. Wulf J, Guckenberger M, Haedinger U, *et al*. Stereotactic radiotherapy of primary liver cancer and hepatic metastases. *Acta Oncol* 2006;45:838–847.
18. Fritz P, Kraus HJ, Muhlnickel W, *et al*. Stereotactic, single-dose irradiation of stage I non-small cell lung cancer and lung metastases. *Radiat Oncol* 2006;1:30.
19. Hara R, Itami J, Kondo T, *et al*. Clinical outcomes of single-fraction stereotactic radiation therapy of lung tumors. *Cancer* 2006;106:1347–1352.
20. Wulf J, Haedinger U, Oppitz U, *et al*. Stereotactic radiotherapy for primary lung cancer and pulmonary metastases: A noninvasive treatment approach in medically inoperable patients. *Int J Radiat Oncol Biol Phys* 2004;60:186–196.
21. Lovelock DM, Hua C, Wang P, *et al*. Accurate setup of paraspinal patients using a noninvasive patient immobilization cradle and portal imaging. *Med Phys* 2005;32:2606–2614.
22. Yamada Y, Lovelock DM, Yenice KM, *et al*. Multifractionated image-guided and stereotactic intensity-modulated radiotherapy of paraspinal tumors: A preliminary report. *Int J Radiat Oncol Biol Phys* 2005;62:53–61.
23. International Commission on Radiation Units and Measurements. ICRU report 50: Prescribing, recording, and reporting photon beam therapy. Bethesda: International Commission on Radiation Units and Measurements; 1993. P. 1–72.
24. Kaplan EL, Meier P. Nonparametic estimations from incomplete observations. *Am J Stat Assoc* 1958;53:457–481.
25. Gray R. A class of K-sample tests for comparing the cumulative incidence of a competing risk. *Ann Stat* 1988;16:1140–1154.
26. Wulf J, Hadinger U, Oppitz U, *et al*. Stereotactic radiotherapy of targets in the lung and liver. *Strahlenther Onkol* 2001;177: 645–655.
27. Herfarth KK, Debus J, Wannenmacher M. Stereotactic radiation therapy of liver metastases: Update of the initial phase-I/II trial. *Front Radiat Ther Oncol* 2004;38:100–105.
28. Sperduto PW. A review of stereotactic radiosurgery in the management of brain metastases. *Technol Cancer Res Treat* 2003;2: 105–110.
29. Hof H, Herfarth KK, Munter M, *et al*. Stereotactic single-dose radiotherapy of stage I non-small-cell lung cancer (NSCLC). *Int J Radiat Oncol Biol Phys* 2003;56:335–341.
30. Hall EJ, Giaccia AJ. Radiobiology for the radiologist. 6th ed. New York: Lippincott Williams & Wilkins; 2006.
31. Garcia-Barros M, Paris F, Cordon-Cardo C, *et al*. Tumor response to radiotherapy regulated by endothelial cell apoptosis. *Science* 2003;300:1155–1159.
32. Wu JS, Wong R, Johnston M, *et al*. Meta-analysis of dose-fractionation radiotherapy trials for the palliation of painful bone metastases. *Int J Radiat Oncol Biol Phys* 2003;55:594–605.
33. Katagiri H, Takahashi M, Inagaki J, *et al*. Clinical results of nonsurgical treatment for spinal metastases. *Int J Radiat Oncol Biol Phys* 1998;42:1127–1132.
34. Maranzano E, Bellavita R, Rossi R, *et al*. Short-course versus split-course radiotherapy in metastatic spinal cord compression: Results of a phase III, randomized, multicenter trial. *J Clin Oncol* 2005;23:3358–3365.
35. Patchell RA, Tibbs PA, Regine WF, *et al*. Direct decompressive surgical resection in the treatment of spinal cord compression caused by metastatic cancer: a randomised trial. *Lancet* 2005; 366:643–648.
36. Gerszten PC, Welch WC. Cyberknife radiosurgery for metastatic spine tumors. *Neurosurg Clin North Am* 2004;15: 491–501.
37. Gerszten PC, Burton SA, Ozhasoglu C, *et al*. Stereotactic radiosurgery for spinal metastases from renal cell carcinoma. *J Neurosurg Spine* 2005;3:288–295.
38. Gibbs IC, Kamnerdsupaphon P, Ryu MR, *et al*. Image-guided robotic radiosurgery for spinal metastases. *Radiother Oncol* 2007;82:185–190.
39. Mori Y, Kondziolka D, Flickinger JC, *et al*. Stereotactic radiosurgery for cerebral metastatic melanoma: Factors affecting local disease control and survival. *Int J Radiat Oncol Biol Phys* 1998;42:581–589.
40. Mori Y, Kondziolka D, Flickinger JC, *et al*. Stereotactic radiosurgery for brain metastasis from renal cell carcinoma. *Cancer* 1998;83:344–353.